Steady-State Response of Periodically Supported Structures to a Moving Load

A.V. Metrikine
Faculty of Civil Engineering and Geosciences, Delft University of Technology, Stevinweg 1, P.O. Box 5048, 2628 CN Delft, The Netherlands

A.R.M. Wolfert
Koiter Institute Delft, Delft University of Technology, P.O. Box 50458, 2600 GB Delft, The Netherlands

A.C.W.M. Vrouwenvelder
TNO Building and Construction Research, Lange Kleiweg 5, P.O. Box 49, 2600 AA Delft, The Netherlands

Steady-state vibrations of periodically supported structures under a moving load are analytically investigated. The following three structures are considered: an overhead power line for a train, a long suspended bridge and a railway track. The study is based on the application of so-called 'periodicity condition', which implies that the shape of a structure is repetitive in time with space translation equal to the distance between neighboring supports. Main attention in the paper is paid to the effect of the load velocity on dynamic response of the structures. It is shown that the higher the load velocity, the wider the deflection field. Deflection of structures grows as the load velocity increases. This grow, however, can be not monotonical due to appearance of critical velocities related to resonances on sub-harmonics of a periodic structure.

Keywords: **dynamics, moving load, periodicity condition, waves, resonance.**

1 Introduction

With the intensive development of high-speed trains it becomes necessary to study the dynamic behavior of rails, overhead power lines, bridges and guide-ways for magnetically levitated vehicles under a moving train. All these structures are periodically supported: rails by sleepers, power lines as well as suspended bridges by suspensions, guide-ways by columns. So, a train always moves along a periodically supported structure and, therefore, it is of clear practical importance to investigate the dynamic response of such structures to a moving load.

In this paper we analytically investigate the steady-state response of periodically supported structures to a uniformly moving constant point load. The following structures are considered: an overhead power line, a long suspended bridge and a railway track. All of them can be studied by using the same method, based on the application of so-called periodicity condition [1, 14, 15]. This method

allows obtaining the steady-state solution in the form of a single Fourier integral. One should notice that there are other general methods, which can be applied to analyze the problem. For example, the Fourier-series techniques [4, 7–9] or the approach based on the Flouquet's theorem [2, 3, 10, 12]. All these methods give similar results and the reason to choose the 'periodicity condition method' is that this method seems to be more elegant.

The paper consists of three sections. In the first section we deal with vibrations of a single-level catenary. It is modeled by an infinitely long string hanged on periodically spaced discrete suspensions. Suspensions are assumed to be equivalent and composed by spring, mass and damper. Taking the advantage of this simple model, we carefully explain here the 'periodicity condition method', which will be also used in the next two sections. Concerning the results of the study, main attention is paid to the dependence of the string vertical displacement upon the velocity of the load.

The second section deals with the response of a long, periodically suspended bridge. The bridge is modeled by an infinitely long Timoshenko beam hanged on discrete identical suspensions. It is assumed that each suspension is a mass-spring-damper system, reacting against the vertical displacement of the beam. Like in the previous section, we are focused here on variation of the beam response with changing of the load velocity.

The last section is devoted to vibrations of a railroad track. As the model we consider a Timoshenko beam on discrete, periodically spaced supports, which are mounted to elastic half-space. It is shown that the half-space can be replaced by a set of identical springs placed under each support of the beam. The equivalent stiffness of these springs is a function of the frequency of the beam vibrations and of the phase shift between vibrations of neighboring supports. By this replacement the model becomes one-dimensional and can be analyzed with the help of the periodicity condition method. In this paper we do not pay attention to the analysis of the beam displacement, but focus on the crucial role of Raleigh waves in the response of the system.

2 Response of a single-level catenary to a moving pantograph

The electrical supply of trains is delivered by a pantograph, which takes electric power from the overhead contact wire, see Fig. 1. The contact wire is tensioned by an axial force and mounted by droppers to a catenary. Vibrations of the contact wire are primarily caused by the moving pantograph, which provides vertical force acting on the wire.

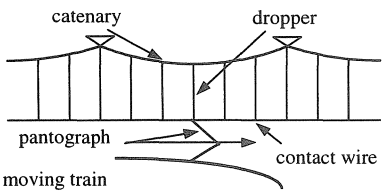

Fig. 1. Electric supply system for a train.

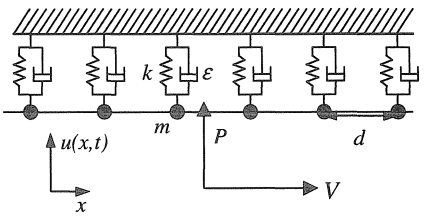

Fig. 2. Model.

To study response of the contact wire we use the model depicted in Figure 2. The model is composed by an infinitely long string and identical mass-spring-damper systems, which are spaced periodically along the string. It is assumed that the pantograph moves along the structure uniformly and acts on it with the constant vertical force P.
The equation of motion for the considered model read as

$$\begin{aligned} &\rho_{str} u_{tt} - N u_{xx} = P\delta(x - Vt) \\ &[u]_{x=nd} = 0 \\ &N[u_x]_{x=nd} = m\ddot{u}_n^0 + \varepsilon \dot{u}_n^0 + k u_n^0 \\ &u_n^0(t) = u(nd, t) \end{aligned} \tag{1}$$

where $u(x, t)$ is the vertical displacement of the string, $u_n^0(t)$ is the vertical displacement of the mass of n^{th} support, n is the number of support (it is assumed that the support $n = 0$ is located at the point $x = 0$), ρ_{str} and N are the mass per unit length and the tension of the string, V is the velocity of the load motion, k, ε and m are the stiffness, viscosity and mass of a support, d is the distance between neighboring supports. The Dirac delta-function is denoted as $\delta(...)$ and the square brackets imply the following difference: $[f(x)]_{x=x_0} = f(x_0 + 0) - f(x_0 - 0)$.
Before starting the analysis of equations (1) we would like to notice that it is invariant with respect to the substitution

$$u(x, t) = u(x + nd, t + nd/V). \tag{2}$$

Equation (2) is normally referred as the **periodicity condition** [1, 14] and implies that the shape of the string is repeated in time with the period $T = d/V$, but with translation in space equal to d.
The advantage of the periodicity condition is clearly seen in the Fourier-domain. To get there one should apply to equations (1) and (2) the following integral transform with respect to time:

$$W(x, \omega) = \int_{-\infty}^{+\infty} u(x, t) \exp(i\omega t) dt.$$

For the equations of motion it yields

$$\begin{aligned} &\frac{\partial^2}{\partial x^2} W + \frac{\omega^2}{c^2} W = -\frac{P}{VN} \exp\left(i\frac{\omega x}{V}\right), \qquad c = \sqrt{N/\rho_{str}} \\ &[W]_{x=nd} = 0 \\ &N\left[\frac{\partial}{\partial x} W\right]_{x=nd} = W(nd, \omega)(k - i\varepsilon\omega - m\omega^2), \end{aligned} \tag{3}$$

while the periodicity condition takes the form

$$W(x + nd, \omega) = W(x, \omega) \exp\left(ind\frac{\omega}{V}\right). \tag{4}$$

Now one can see that, according to periodicity condition (4), the Fourier-displacement of the string in any cell $x \in [nd, (n+1)d]$ can be obtained just by multiplying the Fourier-displacement in interval $x \in [0, d]$ to the factor $\exp(ind\omega/V)$.

Therefore, to solve system (3) one has to make the following steps:

1. Write down the general solution for the Fourier-displacement $W(x,\omega)$ in the interval $x \in [0, d]$. This solution will contain two unknown constants.
2. Using the periodicity condition, obtain an expression for $W(x,\omega)$ in the interval $x \in [nd, (n+1)d]$, which will contain the same two constants.
3. Using two boundary conditions at the point $x = d$ find out the unknown constants.

Let us accomplish the above mentioned steps. The general solution of the first equation of system (3) in the interval $x \in [0, d]$ can be written in the form

$$W(x,\omega) = A\exp\left(\frac{i\omega x}{c}\right) + B\exp\left(-\frac{i\omega x}{c}\right) + S\exp\left(ix\frac{\omega}{V}\right), \tag{5}$$

where $S = -\dfrac{(PV)/\rho_{str}}{\omega^2(V^2 - c^2)}$, A and B are unknown constants.

Then, according to the periodicity condition (4), the solution for $x \in [nd, (n+1)d]$ is given as

$$W(x,\omega) = \exp\left(ind\frac{\omega}{V}\right)\left(A\exp\left(i\omega\frac{x-nd}{c}\right) + B\exp\left(-i\omega\frac{x-nd}{c}\right)\right) + S\exp\left(ix\frac{\omega}{V}\right). \tag{6}$$

Employing finally the boundary conditions at $x = d$ (the second and the third equations of (3) for $n = 1$) and introducing denotations

$$p = \exp\left(id\frac{\omega}{V}\right),\ g = \exp\left(i\frac{\omega d}{c}\right),\ Q(\omega) = k - i\varepsilon\omega - m\omega^2,$$

one obtains the following system of linear algebraic equations with respect to A and B:

$$\begin{cases} A(g-p) + B(1/g - p) = 0 \\ A(i\omega p - i\omega g - pQ(\omega)) + B(-i\omega p + i\omega/g - pQ(\omega)) = -pSQ(\omega). \end{cases}$$

When solved this system gives

$$\begin{aligned} A &= SQ(\omega)\left(\exp\left(id\frac{\omega}{V}\right) - \exp\left(-i\frac{\omega d}{c}\right)\right)/(2i\Delta) \\ B &= SQ(\omega)\left(\exp\left(i\frac{\omega d}{c}\right) - \exp\left(-id\frac{\omega}{V}\right)\right)/(2i\Delta), \\ \Delta &= \omega[(\cos(\omega d/c) - \cos(\omega d/V))2N/c - \sin(\omega d/c)Q(\omega)/\omega]. \end{aligned} \tag{7}$$

Thus, the solution of the problem in the Fourier domain has been obtained. Applying now the inverse Fourier transform to equation (6) and taking into account expressions (7), one can write the solution of problem (1) in the following form:

$$u(x,t) = \frac{1}{2\pi}\Re\left(\int_{-\infty}^{+\infty}\frac{S}{\Delta}I(\omega)\exp(-i\omega t)d\omega\right),$$
$$I(\omega) = Q(\omega)\exp\left(ind\frac{\omega}{V}\right)\left(\exp\left(ind\frac{\omega}{V}\right)\sin\frac{\omega(x-nd)}{c} - \sin\frac{\omega(x-(n+1)d)}{c}\right) + \Delta\exp\left(ix\frac{\omega}{V}\right), \quad (8)$$

where n should be taken equal to the integer part of coordinate x.

To evaluate integral (8) one can use two approaches. First one is the direct numerical integration. Applying this method one has to be careful with zeroes of function $\Delta(\omega)$ (being transcendent, it has infinitely many zeroes), since they give substantial amplification of the integrand. The other approach is the contour integration method [6], which seems to be more relevant here due to the following reasons:

1. The viscosity ε of suspensions is relatively small, therefore, the integrand in eq. (8) is a quasi-singular function due to a number of almost real zeroes of equation $\Delta = 0$. Moreover, this equation has purely real zeroes, which are related to so-called pin-pin mode [6] (this mode occurs when a wave, generated by the load has nodes in the supported points).
2. The integrand converges not so fast (proportionally to ω^{-2}) as $|\omega| \to \infty$. Therefore, to accomplish an accurate direct integration, one has to take into account quite high frequencies, for which the integrand is quickly oscillating.

The contour integration of eq. (8) is carried out as follows. According to the Residue theorem [6] one can write

$$\oint_C \frac{S}{\Delta}I(\omega)\exp(-i\omega t)d\omega = \pm 2\pi i\sum_{k=1}^{n} res_{\Delta}(\omega_k), \quad (9)$$

where C is a closed contour in the complex ω-plane, ω_k are complex roots of equation $\Delta = 0$ lying inside this contour, plus and minus signs are respectively related to clock-wise and anti-clock wise contour integration.

Following now the Jordan's lemma [6], we can close our initial contour (straight line along the real axis of complex ω-plane) by means of a semi-circle with infinite radius, located either in the upper or lower half-plane of ω-plane. The half-plane is to be chosen in order that the integration along the semi-circle vanishes. It can be shown that this requirement is met in the upper half-plane for $x > Vt$ and in the lower one for $x < Vt$. Accounting, additionally, that all zeroes of equation $\Delta = 0$ are simple, one can write the following equality

$$\oint_{-\infty}^{\infty}\frac{S}{\Delta}I(\omega)\exp(-i\omega t)d\omega = \pm 2\pi i\sum_{k=1}^{n}\left.\frac{SI(\omega)\exp(-i\omega t)}{\partial\Delta/\partial\omega}\right|_{\omega=\omega_k}. \quad (10)$$

To calculate the string displacement before the load ($x > Vt$) one has to take in eq.(10) the positive sign and summarize with respect to zeroes ω_k, having a positive imaginary part. Behind the load, respectively, one should use the minus sign and zeroes with a negative imaginary part.

The calculations have been carried out for the following set of the catenary parameters:

$$N = 10^4 \text{ N}, \rho_{str} = 1 \text{ kg/m}, c = 100 \text{ m/s}, P = 100 \text{ N},$$
$$d = 5 \text{ m}, k = 2000 \text{ N/m}, \varepsilon = 20 \text{ sN/m}, m = 0.5 \text{ kg}. \quad (11)$$

Obtained string patterns are depicted in Figures 3(a–d) for four different load velocities. The displacements are given in millimeters and shown at $t = d/(2V)$, when the load is located in the middle of the first span. The distance from the load is given as the dimensionless ratio $\xi = (x - Vt)/d$, therefore, the load is located in the point $\xi = 1/2$ and supports are in the points $\xi = n$, $n = 0, \pm 1, \pm 2, \ldots$ The location of supports is marked in Figures by vertical dashed lines.

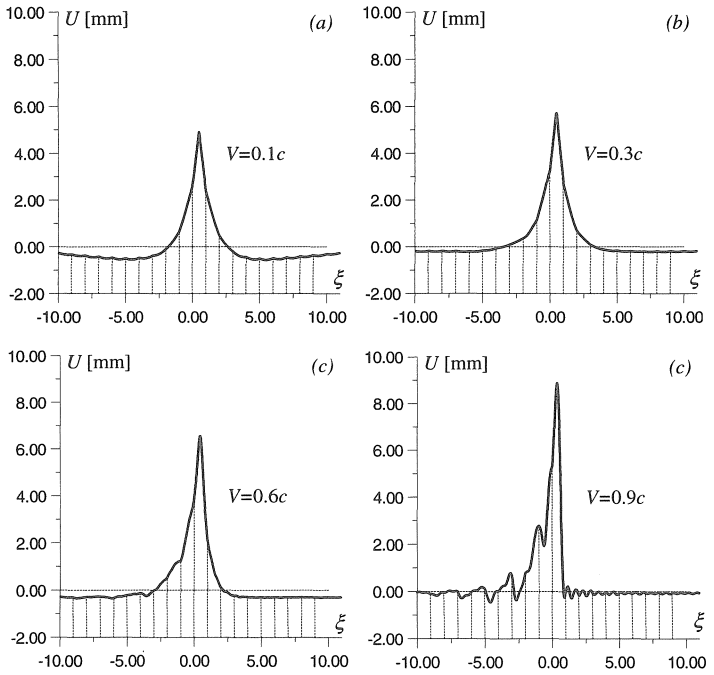

Fig. 3 (a-d). Displacement of the string versus distance from the load.

Analyzing the figures, one can draw the following conclusions:

1. When the load velocity is relatively small ($V = 0.1c$, $V = 0.3c$), the string pattern is almost symmetric with respect to the loading point. With increasing velocity the pattern becomes more and more asymmetric and for $V = 0.9c$ the string displacement before the load becomes negligibly small.
2. Maximum displacement of the string grows, as the load velocity becomes higher.

To demonstrate the last conclusion more clearly, in Figure 4 the dependence of the string displacement in the loading point ($t = d/(2V)$) upon the ratio of load velocity and wave velocity is depicted. For calculation we have used the parameter set (11) varying, however, the viscosity of supports ε. To show the effect of viscosity we considered $\varepsilon = 2$ sN/m and $\varepsilon = 40$ sN/m.
One can see from the Figure that for both values of viscosity the displacement in the loading point substantially grows, as the load velocity increases. The effect of viscosity is noticeable only at velocities of motion close to the wave velocity c.

In Figure 5 the effect of support's mass and stiffness is shown. The thick curve is plotted for the parameters from set (11), but with $k = 20000$ N/m (ten times larger than in Figure 4). For the thin line we additionally increased the mass, taking $m = 5$ kg.

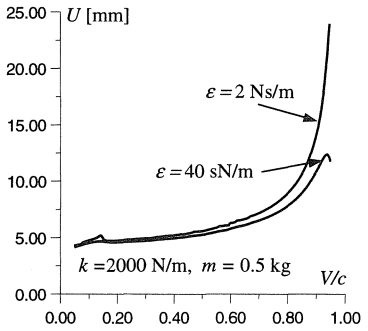

Fig. 4. Displacement under the load vs. velocity for different values of viscosity.

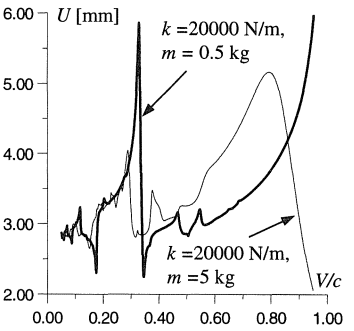

Fig. 5. Effect of the mass and the stifness of supports.

Comparing Figure 5 and Figure 4, one can see that by increasing stiffness of the supports we (fully predictably) reduce the string displacement. Additionally, however, we obtain extra critical velocities, which are related to resonances on sub-harmonics radiated by the load (see [14]). The effect of the mass is most powerful at high velocities of the load, where the increase of the mass substantially reduces the string displacement. Such behavior can be of interest for nowadays operating high-speed trains since they can simply reach the wave velocity in overhead power lines, which is in the order of 300–350 km/h.

3 Response of a suspended bridge

A long suspended bridge (Fig. 6), as well as the catenary, can be approximately described by an infinitely long elastic system on periodic supports (Fig. 7).

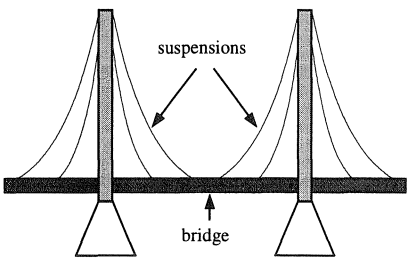

Fig. 6. Suspended bridge.

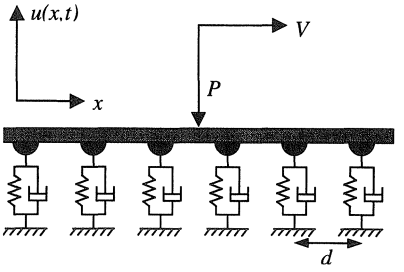

Fig. 7. Model of the bridge subjected to a moving load.

In this chapter we model the bridge by the Timoshenko beam, suspensions by identical mass-spring-damper systems and the train by uniformly moving point load P.

The governing equations describing steady-state vibrations of this system read

$$\begin{aligned}
&\rho F u_{tt} + \gamma_1 u_t - \chi GF(u_{xx} - \varphi_x) = -P\delta(x - Vt)\\
&\rho I \varphi_{tt} + \gamma_2 \varphi_t - EI\varphi_{xx} + \chi GF(\varphi - u_x) = 0\\
&\chi GF[u_x]_{x=nd} = (mu_{tt} + \varepsilon u_t + ku)_{x=nd}\\
&[u]_{x=nd} = [\varphi]_{x=nd} = [\varphi_x]_{x=nd} = 0,
\end{aligned} \tag{12}$$

where $u(x, t)$ is the deflection of the beam neutral line, $\varphi(x,t)$ is the angle of the beam cross-section rotation, ρ is the density of the beam, F is the cross-sectional area, I is the second moment of the cross-sectional area about the neutral axes, E and G are the Young's and the shear modulus of the beam material, γ_1 and γ_2 are the viscosity coefficients, χ is the Timoshenko coefficient, m, ε and k are the mass, viscosity and stiffness of a support, d is the distance between neighboring supports. Other denotations are kept the same as in the previous section. Let us note that the damping in the beam is described by the operator $\gamma_{1,2}\partial/\partial t$, but not by the operator $\gamma_{1,2}\partial^3/\partial t\partial x^2$ which follows from the Voight model of the internal friction. This is done for simplicity, taking into account that in slightly damped systems both operators lead to almost the same result.
Introducing dimensionless variables and parameters as

$$\begin{aligned}
&\alpha = VN/c_s, c_s\sqrt{\chi G/\rho}, y = x/d, \qquad \tau = tc_s/(dN), \qquad U = u/d,\\
&R = \frac{I}{Fd^2N^2}, c^2 = \frac{EI}{\chi GFd^2}, \Gamma_1 = \frac{\gamma_1 dN}{\rho Fc_s}, \Gamma_2 = \frac{\gamma_2}{d\rho FNc_s},\\
&\tilde{P} = \frac{PN^2}{\rho Fc_s^2}, M = \frac{m}{\rho FdN}, K = \frac{kd}{\chi GF}, E = \frac{\varepsilon c_s}{\chi GFN},
\end{aligned}$$

one can rewrite eq.(12) in the form

$$\begin{aligned}
&U_{\tau\tau} + \Gamma_1 U_\tau - N^2(U_{yy} - \varphi_y) = -\tilde{P}\delta(y - \alpha\tau)\\
&R\varphi_{\tau\tau} + \Gamma_2\varphi_\tau - c^2\varphi_{yy} + \varphi - U_y = 0\\
&[U_y]_{y=n} = (MU_{\tau\tau} + EU_\tau + KU)_{y=n}\\
&[U]_{y=n} = [\varphi]_{y=n} = [\varphi_y]_{y=n} = 0,
\end{aligned} \tag{13}$$

where $N > 1$ is a real value, which was introduced to make the dimensionless load velocity α not so small for practical values of the shear wave velocity in a bridge (normally c_s is in the order of 2500–3000 m/s).
System of equations (13) can be analyzed in the same way as it was done for eq. (1) in the previous section. This is due to the fact that the periodicity condition (2) is again valid here, but in the dimensionless and extended to the case of two variables form:

$$U(y, \tau) = U(y + n, \tau + n/\alpha), \qquad \varphi(x, \tau) = \varphi(y + n, \tau + n/\alpha). \tag{14}$$

Following the periodicity condition method, we first apply to eq. (13) and eq. (14) the Fourier transforms over time

$$W(y, \omega) = \int_{-\infty}^{+\infty} U(y, \tau)\exp(i\omega\tau)d\tau, \qquad \Phi(y, \omega) = \int_{-\infty}^{+\infty} \varphi(y, \tau)\exp(i\omega\tau)d\tau.$$

It yields

$$
\begin{aligned}
&N^2(W_{yy}-\Phi_y)+(\omega^2+i\omega\Gamma_1)W = \frac{\tilde{P}}{\alpha}\exp\left(\frac{i\omega y}{\alpha}\right)\\
&c^2\Phi_{yy}-\Phi+W_y+(R\omega^2+i\omega\Gamma_2)\Phi = 0\\
&[W_y]_{y=n} = W(n)(K-iE\omega-M\omega^2) = W(n)Q(\omega)\\
&[W]_{y=n} = [\Phi]_{y=n} = [\Phi_y]_{y=n} = 0
\end{aligned}
\tag{15}
$$

and

$$
W(y+n,\omega) = W(y,\omega)\exp\left(in\frac{\omega}{\alpha}\right),\ \Phi(y+n,\omega) = \Phi(y,\omega)\exp\left(in\frac{\omega}{\alpha}\right).
\tag{16}
$$

Now, analogously to the previous section, one has to find a general solution of first two equations of system (15) in the interval $y\in[0,1]$. This solution can be written as

$$
\begin{aligned}
&W(y) = W^e(y)+S_W\exp(iy\omega/\alpha)\\
&\Phi(y) = \Phi^e(y)+S_\Phi\exp(iy\omega/\alpha),
\end{aligned}
\tag{17}
$$

where

$$
\begin{aligned}
&W^e(y) = A_1\exp(ik_1y)+A_2\exp(-ik_1y)+A_3\exp(ik_2y)+A_4\exp(-ik_2y)\\
&\Phi^e(y) = A_1\beta_1\exp(ik_1y)+A_2\beta_1\exp(-ik_1y)+A_3\beta_2\exp(ik_2y)+A_4\beta_2\exp(-ik_2y),\\
&k_1 = \sqrt{\omega N^2(R\omega+i\Gamma_2)+\omega c^2(\omega+i\Gamma_1)+\sqrt{D}}/(Nc\sqrt{2}),\\
&k_1 = \sqrt{\omega N^2(R\omega+i\Gamma_2)+\omega c^2(\omega+i\Gamma_1)-\sqrt{D}}/(Nc\sqrt{2}),\\
&D = \omega^2(N^2(R\omega+i\Gamma_2)-\omega c^2(\omega+i\Gamma_1))^2+4N^2c^2\omega(\omega+i\Gamma_1),\\
&\beta_{1,2} = ik_{1,2}N^2/(\omega^2+i\omega\Gamma_1-N^2k_{1,2}^2),\\
&S_W = \Delta_W/\Delta_{W\Phi},\qquad S_\Phi = \Delta_\Phi/\Delta_{W\Phi},\\
&\Delta_{W\Phi} = N^2c^2k_L^4-k_L^2(\omega N^2(R\omega+i\Gamma_2)+\omega c^2(\omega+i\Gamma_1))+\omega(\omega+i\Gamma_1)(R\omega^2+i\omega\Gamma_2-1),\\
&\Delta_W = \tilde{P}(R\omega^2+i\omega\Gamma_2-1-c^2k_L^2)/\alpha,\qquad \Delta_\Phi = -i\tilde{P}k_L/\alpha,\qquad k_L = i\omega/\alpha.
\end{aligned}
$$

and $A_j (j=1..4)$ are unknown constants.
Then, according to the periodicity condition (16), the solution in the interval $y\in[n,(n+1)]$ is given as

$$
\begin{aligned}
&W(y) = W^e(y-n)\exp(in\omega/\alpha)+S_W\exp(iy\omega/\alpha)\\
&\Phi(y) = \Phi^e(y-n)\exp(in\omega/\alpha)+S_\Phi\exp(iy\omega/\alpha).
\end{aligned}
\tag{18}
$$

To find out unknown constants $A_j (j=1..4)$ we apply four boundary conditions (third and forth equations of system (15)) at the point $y=1$. Substituting expressions (17) and (18) into these conditions, one obtains

$$
\begin{aligned}
&A_1(g_1-p)+A_2(1/g_1-p)+A_3(g_2-p)+A_4(1/g_2-p) = 0\\
&A_1\beta_1(g_1-p)+A_2\beta_1(p-1/g_1)+A_3\beta_2(g_2-p)+A_4\beta_2(p-1/g_2) = 0\\
&A_1(ik_1p-ik_1g_1-pQ)+A_2(ik_1/g_1-ik_1p-pQ)+A_3(ik_2p-ik_2g_2-pQ)+A_4(ik_2/g_2-ik_2p-pQ) = pQS_W
\end{aligned}
$$

$$A_1\beta_1(ik_1p - ik_1g_1) + A_2\beta_1(ik_1p - ik_1/g_1) + A_3\beta_2(ik_2p - ik_2g_2) + A_4\beta_2(ik_2p - ik_2/g_2) = 0,$$
$$p = \exp(i(\omega + \tilde{\Omega})/\alpha),\ g_{1,2} = \exp(ik_{1,2}).$$

When solved for A_j ($j = 1..4$) this system of linear algebraic equations gives

$$A_j = 4QS_W\Delta_j/\Delta,$$
$$\Delta = a_0\cos(2k_L) - 2b_0\cos(k_L) - c_0$$
$$a_0 = 4(\beta_2k_1 - \beta_1k_2),$$
$$b_0 = 16(\beta_2k_1 - \beta_1k_2)\cos(0.5(k_1 - k_2))\cos(0.5(k_1 + k_2)) + 4Q(\beta_2\sin(k_1) - \beta_1\sin(k_2))$$
$$c_0 = -8(\beta_2k_1 - \beta_1k_2)(1 + \cos(k_1 + k_2) + \cos(k_1 - k_2))$$
$$+ 4Q(\beta_1(\sin(k_2 - k_1) + \sin(k_1 + k_2)) + \beta_2(\sin(k_2 - k_1) - \sin(k_1 + k_2))),$$
$$\Delta_1 = \beta_2\sqrt{p/g_1}\left(\sin\left(\frac{3k_L + k_1}{2}\right) + \sin(k_1)\cos\left(\frac{k_L + k_1}{2}\right) - (\cos(k_1) + 2\cos(k_2))\sin\left(\frac{k_L + k_1}{2}\right)\right),$$
$$\Delta_2 = \beta_2\sqrt{pg_1}\left(-\sin\left(\frac{3k_L - k_1}{2}\right) + \sin(k_1)\cos\left(\frac{k_L - k_1}{2}\right) + (\cos(k_1) + 2\cos(k_2))\sin\left(\frac{k_L - k_1}{2}\right)\right),$$
$$\Delta_3 = \beta_1\sqrt{p/g_2}\left(\sin\left(\frac{3k_L + k_2}{2}\right) + \sin(k_2)\cos\left(\frac{k_L + k_2}{2}\right) - (\cos(k_2) + 2\cos(k_1))\sin\left(\frac{k_L + k_2}{2}\right)\right),$$
$$\Delta_4 = \beta_1\sqrt{pg_2}\left(\sin\left(\frac{3k_L - k_2}{2}\right) - \sin(k_2)\cos\left(\frac{k_L - k_2}{2}\right) - (\cos(k_2) + 2\cos(k_1))\sin\left(\frac{k_L - k_2}{2}\right)\right).$$

Thus, the solution of system (15) has been obtained. Applying now the inverse Fourier transform to equations (18), we obtain the steady-state solution of system (15) in the form

$$U(y,\tau) = \frac{1}{2\pi}\Re\left(\int_{-\infty}^{+\infty}(W^e(y-n)\exp(in\omega/\alpha) + S_W\exp(iy\omega/\alpha))\exp(-i\omega\tau)d\omega\right),$$
$$\varphi(y,\tau) = \frac{1}{2\pi}\Re\left(\int_{-\infty}^{+\infty}(W^e(y-n)\exp(in\omega/\alpha) + S_W\exp(iy\omega/\alpha))\exp(-i\omega\tau)d\omega\right). \quad (19)$$

In contrast to expression (8), it is more convenient to evaluate integrals in expressions (19) by using the direct numerical integration. This is due to the fact that integrands in (19) are quickly vanishing ($N\omega^{-4}$) as $|\omega| \to \infty$ and realistic values of viscosity remove all singularities from the integrands. We have calculated the beam displacements for the following set of parameters:

$$E = 2\cdot10^{11}\ \mathrm{N/m^2},\ G = 7.7\cdot10^{11}\ \mathrm{N/m^2},\ \rho = 8000\ \mathrm{kg/m^3},\ \chi = 0.82,\ (c_s = 2808\ \mathrm{m/s}),$$
$$P = 10^4\ \mathrm{N},\ F = 1\ \mathrm{m^2},\ I = 0.25\mathrm{m^2},\ d = 10\mathrm{m},\ m = 2000\ \mathrm{kg},\ q = -10^6\ \mathrm{kg/s^2} \quad (20)$$
$$\varepsilon = 10^4\ \mathrm{kg/s},\ \gamma_1 = 10^4\ \mathrm{kg/(ms)},\ \gamma_2 = 10^4\ \mathrm{Ns}.$$

As one can see, in the considered case the shear wave velocity is about 2800 m/s. Evidently, velocities of nowadays operating trains are incomparably smaller (the ratio V/c_s is at maximum of the order of 0.03). Therefore, to make the dimensionless velocity $\alpha = V/(Nc_s)$ comparable to the unity, which is necessary to improve the accuracy of calculations, we take the dimensionless factor N equal to 10.

In Figure 8 the displacements of the beam neutral line are depicted versus dimensionless distance from the load $\xi = (x - Vt)/d$ for four different magnitudes of the load velocity (the distance between neighboring suspensions in the chosen scale is equal to unity). Vertical and horizontal dashed lines in the Figure respectively show the instant position of the load and the position of the undisturbed neutral line.

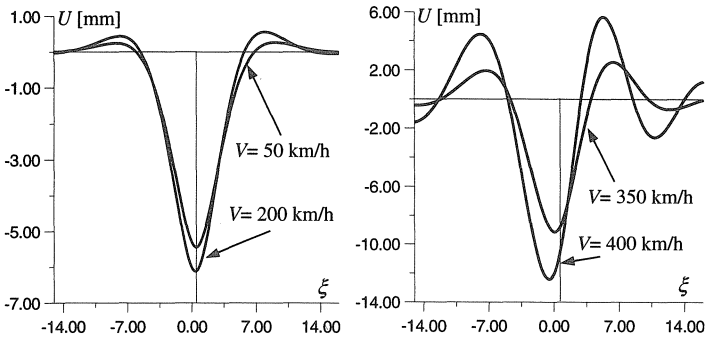

Fig. 8. Displacements of the beam neutral line versus dimensionless distance from the load.

One can see from the Figure that for relatively small velocities of the load (50 km/h and 200 km/h) the beam displacement pattern is almost symmetric with respect to the loading point and is localized around this point. The localization, however, is relative since the beam displacement is perceptible within at least 10 spans from the load.

For higher load velocities the beam pattern becomes rather asymmetric and 'wave-like'. The higher the velocity of the load, the wider the displacement field is spread.

The similar conclusions can be drawn for the moments in the beam, which are depicted in Figure 9 as a function of ξ for different velocities of the load (the moments are related to the rotational angle as $M = -EI\varphi_x$).

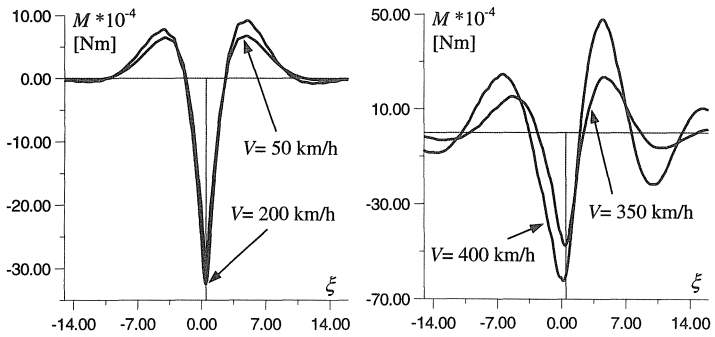

Fig. 9. Moments versus dimensionless distance from the load.

Both Figure 8 and Figure 9 show that the beam deflection grows as the load velocity increases. This effect is explicitly depicted in Figure 10 where the instant displacement of the beam under the load ($x = d/2$, $t = \mathrm{d}/(2V)$) is plotted versus the load velocity.

It is obvious from the Figure that the beam displacement under the load has a maximum when the load velocity is about $V^* \approx 400$ km/h. One can easily show that this velocity corresponds to the smallest phase velocity of waves in the beam. When the velocity exceeds V^*, the load starts radiating waves into the beam and the maximum displacement is not anymore located in the loading point. So, the decrease of the displacement in the loading point, which takes place for $V > V^*$ should not be understood as the decrease of the maximum beam displacement.
Concerning the effect of the suspension parameters one can say that the mass and the viscosity have a slight influence in the considered velocity range. By increasing the stiffness of the suspension one can substantially reduce the beam deflection. In contrast to the catenary case, the increase of the stiffness does not bring here any new perceptible resonances.

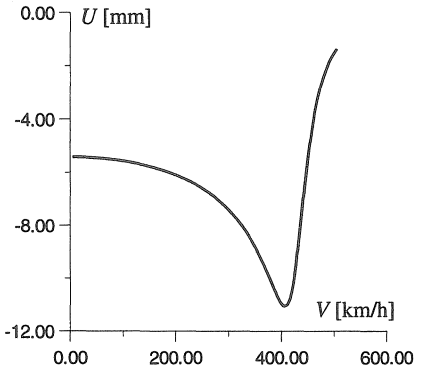

Fig. 10. Displacement under the load versus velocity.

4 Response of rails to a moving train

In this section we analyze the dynamic response of a railroad track to a moving train, taking into account the coupling between rails, sleepers and the track subsoil, see Figure 11.

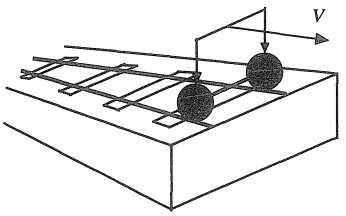

Fig. 11. Train motion along a railroad track.

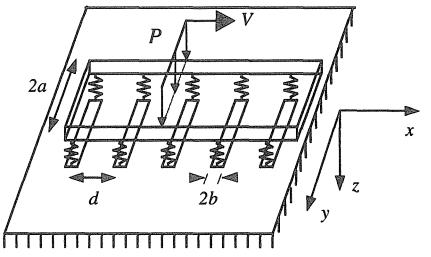

Fig. 12. Model, composed by a beam, discrete supports and a half-space.

To study the response of the track we consider a uniform motion $x = Vt$ of a harmonically varying vertical load P along a Timoshenko beam, resting on periodically spaced discrete elastic supports, which are based on an elastic half-space as depicted in Figure 12.
The model is analyzed under the following assumptions: 1) the beam has finite width $2a$, but vibrates as one-dimensional system; 2) the contact area between each support and the half-space is supposed to be flat and rectangular of the size $2a$ x $2b$. The contact is smooth, hence the shear stresses τ_{xz} and τ_{yz} are zero at the interface. The normal stress σ_{zz} is uniformly distributed beneath the contact area; 3) all supports are equal and consist of a mass-spring system. The mass m is concentrated at the middle point of the contact area. The visco-elastic element of total stiffness k and viscosity ε connects the contact area and the beam and is uniformly distributed over the beam width; 4) the load is uniformly distributed over the beam width. Let us note that the assumption about the vanishing of the shear stresses at the interface can not be exactly fulfilled in reality. However, taking into account that the dynamics of the structure is almost fully determined by relatively long waves (see [5]), application of this assumption does not lead to a perceptible error.

With these assumptions the governing equations of motion can be written as

– The equations of motion of the half-space in terms of so-called stress functions $\varphi(x, y, z, t)$ and $\psi(x, y, z, t)$, see [5]:

$$\Delta\varphi = \frac{1}{c_L^2}\frac{\partial^2}{\partial t^2}\varphi, \qquad \Delta\psi = \frac{1}{c_T^2}\frac{\partial^2}{\partial t^2}\psi, \tag{21}$$

where $c_L = \sqrt{(\lambda + 2\mu)/\rho_{hs}}$ and $c_T = \sqrt{\mu/\rho_{hs}}$ are the velocities of the compression and shear waves, respectively, λ and μ are the Lamé constants for the elastic half-space and ρ_{hs} is its mass density, Δ is the Laplace operator.

– The balance of stresses at the surface of the half-space $z = 0$:

$$\begin{aligned}
&\sigma_{zz}(x, y, 0, t) = \frac{1}{4ab}H(a - |y|)\sum_{n=-\infty}^{\infty} H(b - |x - nd|)\times \\
&\left\{k(u^0(nd, t) - u(nd, 0, 0, t)) - \varepsilon\frac{\partial}{\partial t}(u^0(nd, t) - u(nd, 0, 0, t)) - m\frac{\partial^2}{\partial t^2}u(nd, 0, 0, t)\right\}, \\
&\tau_{xz}(x, y, 0, t) = \tau_{yz}(x, y, 0, t) = 0,
\end{aligned} \tag{22}$$

where $u(x, y, z, t)$ and $u^0(x, t)$ are the vertical displacements of half-space and beam, respectively and $H(\,)$ is the Heaviside step function.

– The equations for the beam motion

$$\begin{aligned}
&\rho F u_{tt} + \gamma_1 u_t - \chi GF(u_{xx} - \varphi_x) = -P\delta(x - Vt) \\
&\sum_{n=-\infty}^{\infty}\delta(x - nd)\left\{k(u^0(x, t) - u(x, 0, 0, t)) + \varepsilon\frac{\partial}{\partial t}(u^0(x, t) - u(x, 0, 0, t))\right\}, \\
&\rho I\varphi_{tt} + \gamma_2\varphi_t - EI\varphi_{xx} + \chi GF(\varphi - u_x) = 0.
\end{aligned} \tag{23}$$

where the denotations related to the beam are kept the same as in the previous section.
It is convenient to split the analysis of system (21)–(23) into two steps. First, employing the concept of 'equivalent stiffness' [5], we replace the half-space by equivalent springs with stiffness, depending on the dynamic process in the beam. It can be done exactly by putting identical springs under every support as it is shown in Figure 13.

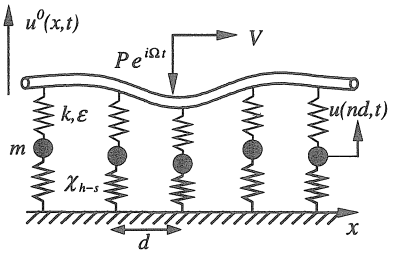

Fig. 13. Equivalent model.

In this case the stiffness χ_{h-s} of equivalent springs is a function of frequency ω of the beam vibrations and a constant phase shift $q(\omega)$ between vibrations of neighboring supports.
The way of obtaining the expression for the equivalent stiffness χ_{h-s} is described in detail in [13]. As it is shown there, the final expression for χ_{h-s} can be written as

$$\chi_{h-s}(\omega, q(\omega)) = \left(\frac{\omega^2}{4\pi^2 \mu c_{T_j}^2} \sum_{j=-\infty}^{\infty} \int_{-\infty}^{\infty} \int_{-\infty}^{\infty} \frac{R_L}{\Delta} \frac{\sin(bk_1)}{bk_1} \frac{\sin(ak_2)}{ak_2} \exp(i(k_1 d - q(\omega))j) dk_1 dk_2 \right)^{-1} \tag{24}$$

where

$$\Delta(k_1, k_2, \omega) = (2(k_1^2 + k_2^2) - \omega^2/c_T^2)^2 - 4R_L R_T (k_1^2 + k_2^2),$$

$$R_{L,T} = \sqrt{k_1^2 + k_2^2 - \omega^2/c_{L,T}^2}$$

The result of the numerical evaluation of expression (24) is qualitatively presented in Figure 14. The equivalent stiffness of the half-space is shown in this Figure as a function of frequency for a fixed phase shift between the support vibrations. Both, the real and the imaginary parts are depicted.

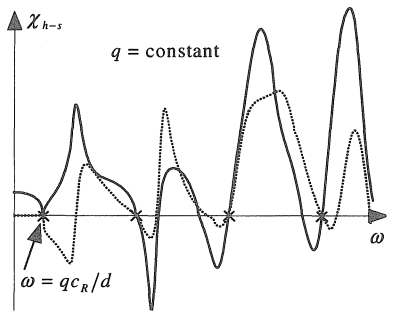

Fig. 14. Real part (solid line) and imaginary part (dashed line) of the equivalent stifness for a constant phase shift q.

One can see from the Figure that the equivalent stiffness is equal to zero for $(\omega d)/c_R = |q(\omega) + 2\pi n|$ (points, marked by crosses). This happens because of Rayleigh waves, which, being radiated by vibrating supports, are summarized in phase at the contact points between the half-space and the supports.

For frequencies smaller than $\omega = qc_R/d$ the imaginary part of the equivalent stiffness is equal to zero. It implies that in this band of frequencies, vibrations of the supports generate no waves in the elastic half-space.

It can be seen further from the figure that the equivalent stiffness can reach quite large magnitudes for some frequencies. This effect can be considered as an 'anti-resonance' when waves, as well as exponentially decaying displacement fields, generated by the supports are summarized at the contact points almost in anti-phase.

Thus, by introduction of the equivalent stiffness, we have reduced the initial three-dimensional model, depicted in Figure 12 to one-dimensional model shown in Figure 13. Now, to find the dynamic response of the beam, the periodicity condition method can be applied in the same way as in the previous section. Moreover, solution of the problem (21)–(23) still can be written in the form (19). The only change, one has to make is to replace $Q(\omega) = (K - iE\omega - M\omega^2)$ (see eq.(15)) by

$$Q(\omega) = \frac{(K - i\omega E)(\hat{\chi}_{h-s} - M\omega^2)}{K - i\omega E + \hat{\chi}_{h-s} - M\omega^2}, \qquad \text{where } \hat{\chi}_{h-s} = \frac{\chi_{h-s} d}{\chi GF}.$$

In this paper we will not pay attention to the analysis of the beam displacement (it should be a subject of separate publication), but focus on the crucial role of Raleigh waves in the response of the track.

If the load is constant, then expression for the phase shift $q(\omega)$ reads as $q(\omega) = \omega d/V$ (see [13]) and, according to Figure 15, the equivalent stiffness vanishes for frequencies

$$\omega d/c_R = |(\omega d)/V + 2\pi n|.$$

It is obviously seen from this equation that if the velocity of the load V is equal to Rayleigh wave velocity c_R, then the equivalent stiffness of the half-space is equal to zero for all frequencies (let $n = 0$). Therefore, if $V = c_R$, then the vertical force acting on the supports from the half-space is equal to zero. This situation leads to an infinite steady-state displacement of the beam.

Thus, the Rayleigh wave velocity is the critical one for a constant load moving along the periodically supported beam on a half-space. This result is of practical importance for nowadays operated high-speed trains since the Rayleigh wave velocity in a track subsoil can be in the order of 250 km/h or even less if the subsoil is soft, see [5].

5 Conclusions

In this paper a general method has been demonstrated of dynamical analysis of periodically supported structures under a moving load. The method is based on application of so-called periodicity condition, which reads as

$$u(x, t) = u(x + nd, t + nd/V),$$

where $u(x, t)$ is the deflection of a structure, x is the space co-ordinate along the structure, t is time, d is the distance between neighboring supports, V is the velocity and the angular frequency of the load, n is an integer. By applying this condition one can obtain analytical expressions for deflections of a structure in the form of single Fourier integral.

Three different structures have been considered in the paper, i.e.: an overhead power line under a moving pantograph, a long suspended bridge under a moving vehicle and a railway track under a moving train. All the structures have been assumed infinitely long and being subjected to uniformly moving harmonic point load.

Main attention in the paper has been paid to the effect of the load velocity on dynamic response of the structures. It has been shown that for relatively small velocities of motion deflection fields in the structures are symmetric with respect to the loading point and localized in its vicinity. As the velocity grows, the fields become more and more asymmetric and the deflection fields get wider. By analyzing the dependence of deflection in the loading point upon the load velocity it has been shown that the deflection grows as the velocity increases. This grow, however, takes place only while the load velocity does not exceed the minimum phase velocity of the main harmonics in a structure (in the power line, for example, this velocity corresponds to the velocity of transverse waves in the cable). Moreover, if the stiffness of the supports becomes larger, the deflections can considerably grow at relatively small velocities. This is especially valid for the overhead power line and related to resonance on sub-harmonics of periodical structures.

In the model of a railway track the subsoil has been taken into account by including elastic half-space as an underlying structure for periodic supports (pads plus sleepers). It has been shown that the Rayleigh wave velocity is the critical one for a constant load moving along such a structure. This result is of special practical importance since in a soft subsoil this velocity can be in the order of 250 km/h or even smaller.

Concluding the paper, we would like to notice that the models used in the paper to describe engineering constructions can be substantially improved. For example, the droppers of the catenary could be much better modeled by non-linear springs than by linear ones because of their different reaction against the up and down motion. The suspended bridge, especially for high velocities of the load motion, should be assumed to have a finite length. The subsoil of a railroad track could be considered as a layered structure, etc.

Despite of all the mention disadvantages, the models considered in the paper posses the main feature of the real constructions, i.e. the periodicity. Therefore, the obtained results are believed to be qualitatively correct.

6 Literature

BELOTSERKOVSKIY P.M., 'On the oscillations of infinite periodic beams subjected to a moving concentrated force', *Journal of Sound and Vibration 193(3)*, 706–712 (1996).

BOGACZ R., KRZYZINSKI T. and POPP K., 'On dynamics of systems modeling continuous and periodic guideways', *Archives of Mechanics 45(5)*, 575–593 (1993).

BOGACZ R., KRZYZINSKI T. and POPP K., 'On the vertical and lateral dynamics of periodic guideways for MAGLEV vehicle', *Dynamical Problems in Mechanical Systems, Proc. 3rd German-Polish Workshop, Wierzba, Poland*, 219–232 (1993).

Cai C.W., Cheung Y.K. and Chan H.C., 'Dynamic response of infinite continuous beams subjected to a moving force - an exact method', *Journal of Sound and Vibration 123(3)*, 461–472 (1988).

Dieterman H.A. and Metrikine A.V., 'The equivalent stiffness of a half-space interacting with a beam. Critical velocities of a moving load along the beam', *European Journal of Mechanics A/Solids 15(1)*, 67–90 (1996).

Fuchs B.A., Shabat B.V., Berry J., *Functions of complex variables and some of their applications*, Oxford, Pergamon (1961–1964).

Genin J., Chung Y.I., 'Response of a continuous guideway on equally spaced supports traversed by a moving vehicle', *Journal of Sound and Vibration 67(2)*, 245–251 (1979).

Jezequel L., 'Analysis of critical speeds of a moving load on an infinite periodically supported beam', *Journal of Sound and Vibration 73(4)*, 606–610 (1980).

Jezequel L., 'Response of periodic systems to a moving load', *ASME Journal of Applied Mechanics 48(3)*, 603–618 (1981).

Krzyzynski T., 'The influence of viscous damping on the dynamics of periodic structures', *ZAMM 73(4)*, T11–T114 (1993).

Mead D.J., 'Vibration response and wave propagation in periodic structures', *ASME J. Engng. for Industry 93(3)*, 783–792 (1971).

Manabe K. 'Periodical dynamic stability's of a catenary-pantograph system', *QR of RTRI 35(2)*, 112–117 (1994).

Metrikine A.V. and Popp K., 'Vibration of a periodically supported beam on an elastic half-space', *European Journal of Mechanics A/Solids 18(4)*, 679–701 (1999).

Vesnitskii A.I. and Metrikine A.V., 'Transient radiation in a periodically non-uniform elastic guide', Mechanics *of solids 28(6)*, 158–162 (1993).

Velten J.J., 'The dynamic behavior of overhead contact wire', Tu-Delft graduation report (1999).